Journal of the European Ceramic Society **15** (1995) 109–116

0955-2219/95/$9.50

Shrinkage and Particle Packing during Removal of Organic Vehicle from Ceramic Injection Mouldings

Heidi M. Shaw & Mohan J. Edirisinghe

Department of Material Technology, Brunel University, Uxbridge, Middlesex, UK, UB8 3PH

(Received 21 February 1994; revised version received 3 June 1994; accepted 30 June 1994)

Abstract

Alumina suspensions, containing 50 and 57 vol.% ceramic in isotactic polypropylene and microcrystalline wax, were prepared by high shear mixing and injection moulded. The test bars produced were heated in air at 5°C h^{-1} to four different temperatures in the range 155–225°C and up to about 25 wt% of organic vehicle was removed. Shrinkage in the bars was measured after cooling to room temperature. The difference in the coefficient of thermal expansion of the suspension during heating and cooling, the changes in the crystallinity of the polypropylene and wax compared with the as-moulded state and the mobility of the ceramic particles due to removal of the organic vehicle are contributory factors to the measured shrinkage. The anticipated dimensional changes due to the first two factors have been determined experimentally and thereby the change in particle packing in the inner regions (core) of the test bars due to the mobility of the ceramic in the suspension have been calculated. Results show that in both suspensions heating to just above the softening point caused appreciable particle packing. Subsequently, particle packing decreases substantially and the reasons for this are discussed, taking into account thermal expansion of the organic vehicle, capillary migration of the microcrystalline wax, loss of organic vehicle and development of porosity. Comparison of results with previous investigations show that particle packing is affected by the rate of heating and the atmosphere used during pyrolysis. Particle packing, during pyrolysis, in the more concentrated suspension (57 vol.% ceramic) was, as expected, smaller, except at 225°C, when the core of each test bar containing this formulation showed a steep increase in weight loss. Otherwise, both formulations show similar trends in particle packing during the initial stages of the removal of organic vehicle.

1 Introduction

A commercially attractive method of producing large numbers of dimensionally accurate complex shap engineering ceramic components is plastic forming ceramic suspensions containing an organic vehicle.[1,2] However, full-scale industrial exploitation of plastic-forming methods (e.g. injection moulding, vacuum forming, blow moulding, film blowing) has not been possible, due to difficulties in removing the organic vehicle from the ceramic prior to sintering, without creating defects.

The organic vehicle can be removed by using solvents or, more frequently, by slow pyrolysis.[3] A decade ago successful use of the latter method was thought to involve mainly careful control of the rate of heating as a function of weight loss.[4] However, as plastic-forming methods were used increasingly to produce components with larger section sizes (>10 mm), it became clear that several factors determined the outcome of the crucial pyrolysis stage. These have been reviewed recently[5] and the major factors are:

(1) The rate of heating and the atmosphere in which pyrolysis is carried out.
(2) Characteristics of the organic vehicle.
(3) Characteristics of the ceramic.
(4) A balance between degradation of the organic vehicle and the outward diffusion of the resulting products.
(5) Formation of porosity.

One important phenomenon that occurs during the removal of organic vehicle by pyrolysis but has not been investigated extensively is the movement of the ceramic particles. It is known that, at the end of the organic vehicle removal stage, shrinkage and an increase in particle packing are observed.[6] Ceramic particles can be drawn towards each other under the influence of capillary forces which arise from the curvature of inter-par-

ticle surface menisci or of internal porosity formed during pyrolysis, much like in the initial stages of liquid-phase sintering.[7] However, during the initial stages of pyrolysis the liquid organic vehicle expands[8,9] and it is suggested[9] that this can result in the development of hydraulic pressures in the suspension with the ceramic particles forming a rigid network preventing further packing. Thermal expansion coefficients of ceramic suspensions can be measured in the liquid and the solid state,[10] indicating that particles are mobile and therefore the hypothesis that they form a rigid network lacks experimental evidence.

It is well known that packing of ceramic particles depends on their characteristics,[11] in particular their shape.[12] In the case of spherical powders, particle centres approach each other and porosity decreases due to the increase in packing. However, most commercial ceramic powders are non-spherical and their motion to enhance packing requires both the approach of particle centres and particle rotation. Removal of the organic vehicle from inter-particle spaces in the suspension can give rise to the former type of movement but the latter could be difficult in a suspension having high viscosity, especially during the initial stages (low temperatures) of pyrolysis. Another factor which could retard rotation of the particles is the presence of immobile layers of adsorbed organic vehicle on the ceramic surfaces.[13]

The measured shrinkage after heating to various temperatures and subsequent cooling to room temperature during pyrolysis of the organic vehicle does not fully correspond to the particle packing that has taken place. Firstly, compared to the heating cycle, the suspension contains a different amount of organic vehicle during cooling to room temperature and this can result in a difference in the coefficient of thermal expansion, causing a dimensional change that has to be taken into account. Secondly, the crystalline polymeric components in the organic vehicle, such as isotactic polypropylene and microcrystalline wax in the present work, can have different percentage crystallinities dependent on thermal history and processing[14,15] and this causes dimensional change. Therefore, the associated dimensional change due to the difference in crystallinity of the relevant constituents in the organic vehicle after heating to various temperatures during pyrolysis and subsequent cooling to room temperature has to be estimated.

Previous investigations[16,17] led to a quantitative assessment of the development of porosity (during the initial stages of pyrolysis in air) in injection-moulded test bars containing 50 and 57 vol.% alumina, suspensions made using an organic vehicle in which isotactic polypropylene and microcrystalline wax were the major and minor constituents, respectively. In the present work, identical ceramic suspensions and test bars are used and pyrolysis has been interrupted at four different temperatures to measure shrinkage after cooling to room temperature. The corresponding dimensional changes due to thermal expansion coefficient and crystallinity already discussed have been calculated from experimental results. Thereby the measured shrinkage has been corrected to calculate the vol.% shrinkage caused by the packing of ceramic particles during the initial stages of pyrolysis when up to 25 wt% organic vehicle is removed.

2 Experimental details

2.1 Production of test bars

Two formulations A and B containing 50 and 57 vol.%, respectively, of A16.SG alumina (Alcoa Manufacturing (GB) Ltd, Worcester, UK) were prepared using an organic vehicle containing isotactic polypropylene (density 905 kg m^{-3}), microcrystalline wax (density 910 kg m^{-3}) and stearic acid in the weight ratio 6:2:1. Further details of the ceramic powder and each constituent in the organic vehicle have been published earlier.[17]

Preblends of formulations A and B were prepared by tumbling the formulations in a container and then compounding in a twin screw extruder (Model TS40, Betol Machinery, Luton, Bedfordshire, UK). Compounding conditions of these formulations have been published previously.[17] The extrudate was dried and granulated, and the ceramic loading was verified by ashing samples (by heating to 600°C).

A 6GV/50 Sandretto reciprocating screw injection-moulding machine was used to produce 3 mm thick tensile test bars (Fig. 1) according to conditions reported previously.[17] The injection pressure, nozzle temperature and mould temperature used were 127MPa, 50°C and 235°C, respectively. The test bars were X-ray radiographed to verify that there were no voids or cracks present after moulding.

2.2 Pyrolysis

Test bars were pyrolysed in a muffle furnace in static air. The rate of heating was determined by trial and error experiments such that pyrolysis does not produce voids or cracks in the mouldings. The bars were heated initially from room temperature to a few degrees below the softening points of the formulations (148°C) at 50°C h^{-1} and then soaked for 24 h at this temperature. Subsequently, heating was continued at 5°C h^{-1}. Three

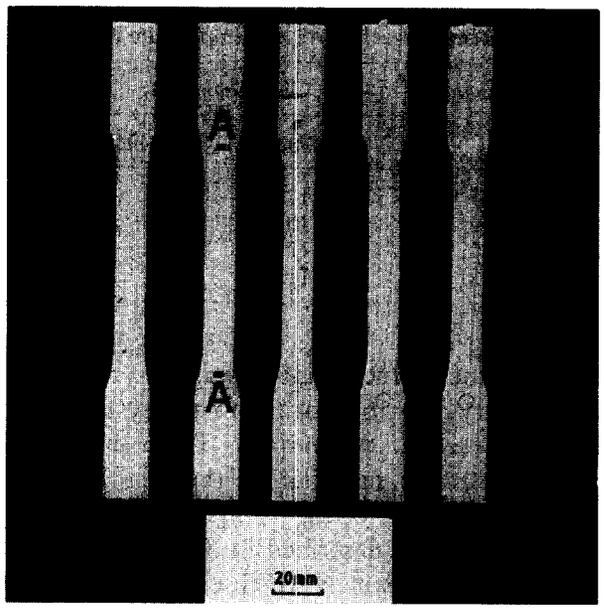

Fig. 1. Injection mouldings produced (nominal thickness 3mm). AA indicates the position and length of the test bars used for measurement of linear shrinkage.

test bars of each formulation were heated to 155, 170, 195 and 225°C (referred to as pyrolysis temperatures in the text and measured to an accuracy of ± 1°C) before cooling in the furnace to room temperature. Test bars were X-ray radiographed after pyrolysis to verify that voids and cracks were absent and subsequently were used to carry out the following experiments in triplicate.

2.3 Measured linear shrinkage

Two marks were scribed on the test bars as shown in Fig. 1 prior to pyrolysis. The distance between the two marks was measured with a travelling microscope before and after pyrolysis to the temperatures given in Section 2.2.

2.4 Loss on ignition

After pyrolysis, the test bars showed a clear contrast in colour between the core and surface regions (Fig. 2). Therefore, the material in the surface region was carefully separated from the core by scoring with a scalpel blade. The dimensions of the core were measured using Vernier callipers to calculate (separately) the vol.% of test bar that constitutes the core and the surface regions as pyrolysis progressed. Samples of both surface and core material were heated to 600°C (in triplicate) to calculate the weight loss of organic vehicle.

2.5 Dilatometry

Thermal expansion curves were obtained for 2·5 × 2·5 mm cross-section core samples (4mm thick) using a Perkin Elmer TMS1 thermomechanical analyser (TMA). Expansion was measured along the length of the test bars. A load of 3 g was used

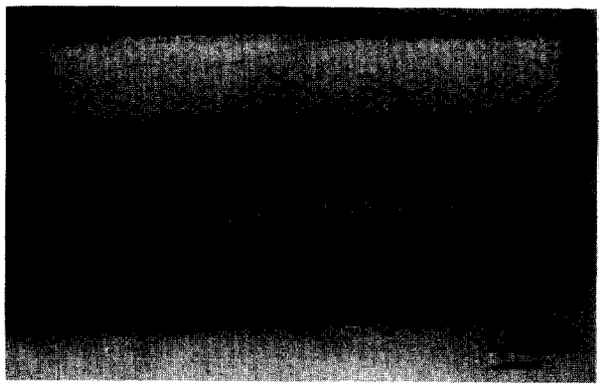

Fig. 2. Typical appearance of the cross-section of test bars after pyrolysis showing the dark surface region. Examples shown are: (a) A test bar of formulation A pyrolysed to 195°C; (b) a test bar of formulation B pyrolysed to 195°C.

on a flat-ended silica glass rod (diameter 4 mm) during heating the samples at $8°C^{-1}$ h to 120°C. These experimental conditions have been used successfully in previous work[18] to calculate the linear thermal expansion coefficient of ceramic suspensions. The TMA was calibrated using a pure sample having a linear thermal expansion coefficient of $2·3 \times 10^{-5}$ K^{-1}.

2.6 Differential scanning calorimetry (DSC)

A Perkin-Elmer DSC2 was used to measure enthalpies of fusion of samples taken from the core of pyrolysed test bars. A scan speed of 10 K min^{-1} was used during heating the samples between room temperature and 250°C.

3 Results and discussion

3.1 Mechanisms of removal of the organic vehicle

The dark appearance of the surface of pyrolysed test bars of both formulations (Fig. 2) suggests that the organic vehicle present in these regions has been subjected to a greater level of degradation compared with the core. This is due to the presence of oxygen in the atmosphere in which pyrolysis is carried out. Oxidative degradation occurs in the surface regions while thermal degradation dominates in the core of the mouldings[19,20] and the former is known to give rise to a higher weight loss at a lower temperature.[21] Loss on ignition results of surface and core samples shown in Fig. 3 indicate an increase in the wt% of organic vehicle in the surface regions at 195 and 225°C in formulation A and at 170°C in formulation B. Therefore, enrichment of the organic vehicle in the surface regions occurred in both formulations (over a wider temperature range in formulation A which contained more organic vehicle) during the initial stages of pyrolysis. The organic vehicle in both surface and core regions of the test bars after

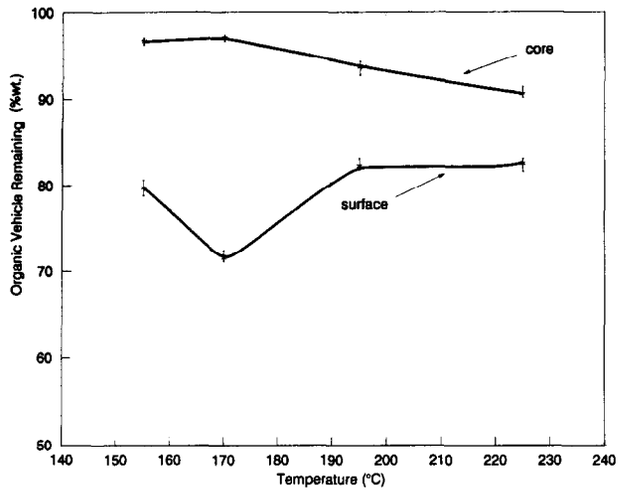

(a)

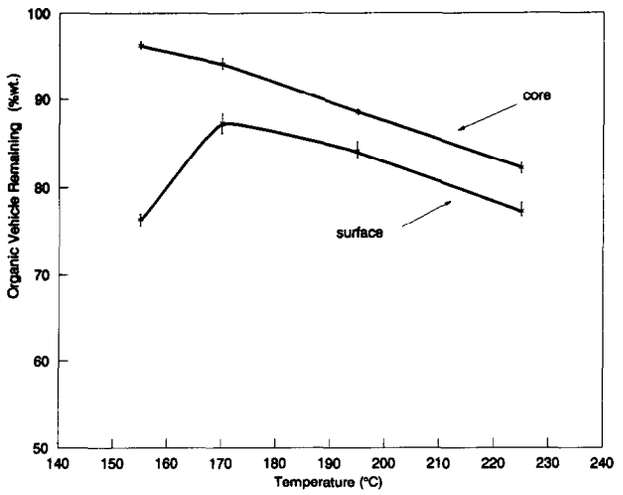

(b)

Fig. 3. Variation of weight of organic vehicle remaining (as a percentage of the initial weight of organic vehicle in the as-moulded test bars) with pyrolysis temperature in the surface region and the core of the mouldings of (a) formulation A; (b) formulation B. Formulations A and B contained 81·24 (±0·05) wt% (equivalent to 49·7 vol.%) and 85·17 (±0·14) wt% (equivalent to 56·7 vol.%) ceramic in the as-moulded state (from ashing at 600°C). Thus the green densities of formulations A and B are 2440 kg m^{-3} and 2655 kg m^{-3}, respectively.

pyrolysis has been analysed by gel permeation chromatography (GPC) and reported previously.[22] GPC results show that the polypropylene in the core of test bars of both formulations did not show any appreciable degradation but the intensity of the wax peak decreased. In contrast, at the surface, although the polypropylene present in the organic vehicle degraded to some extent (particularly at 225°C), the significant feature was the increase in the intensity of the wax peak. Therefore, in the context of the present investigation, the important mechanism of removal of organic vehicle from the core of the test bars of both formulations during the initial stages of pyrolysis is the capillary migration of the microcrystalline wax to the surface.

The rate of weight loss due to oxidative degradation in the surface regions was also affected by the capillary migration of the microcrystalline wax from the core to the surface. The vol.% of discoloured surface material in the test bars (presented in Table 1 using results from the experimental procedure described in Section 2.4) hardly varies in formulation A which contained more organic vehicle and showed capillary migration of microcrystalline wax over a wider temperature range, as already discussed. In contrast, there is a rapid increase in the vol.% of surface material in test bars of formulation B.

Table 1. Volume of test bar which contains discoloured surface material at each pyrolysis temperature investigated

Temperature (°C)	*Volume (%)*	
	Formulation A	*Formulation B*
155	12	6
170	10	13
195	10	19
225	11	22

3.2 Measured shrinkage

The linear shrinkages (S_L) measured (Table 2) were converted to volume shrinkages (S_v) by using the expression:

$$S_v = 3S_L - 3S_L^2 + S_L^3 \quad (1)$$

Figure 4 shows the variation of S_v with pyrolysis temperature. In order to understand further the behaviour of the suspensions during pyrolysis, S_L of the test bars was also measured at 150°C (just below the softening point of both formulations; dilatometric measurements give 151°C (formulation A) and 154°C (formulation B)) and the corresponding S_v values are also shown in Fig. 4. In both formulations S_v increases initially. This is expected as residual stresses are released on heating past the softening point and the ceramic particles have the opportunity to move towards each other as suspensions begin to lose organic vehicle. However, at 170°C both formulations show a decrease in S_v.

Bandyopadhyay & French[8] observed a similar effect during the interrupted pyrolysis of injection-

Table 2. Linear shrinkages (S_L) in test bars of formulations A and B at each pyrolysis temperature

Temperature (°C)	*S_L(%)*	
	Formulation A	*Formulation B*
155	1·24, 1·31, 1·33	0·56, 0·75, 0·85
170	0·68, 0·62, 0·63	0·46, 0·49, 0·46
195	0·59, 0·56, 0·54	0·40, 0·31, 0·38
225	0·20, 0·15, 0·12	0·18· 0·15, 0·18

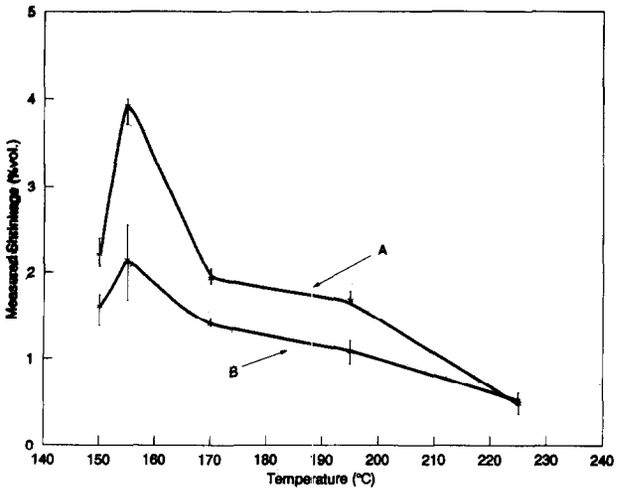

Fig. 4. Variation of measured vol.% shrinkage (S_v) with pyrolysis temperature in formulations A and B. S_v values correspond to the average S_L value of the measurements given in Table 2.

moulded test bars and spheres made using silicon nitride powder and an organic vehicle which contained microcrystalline wax and epoxy resin as the major and minor constituents, respectively. Volume expansion of the organic vehicle takes place during heating but S_L, measured at room temperature, can only show a decrease if the ceramic particles in the core of the mouldings are restrained from moving during cooling. However, S_v values can also be influenced by changes in the properties of organic vehicle during pyrolysis (see Sections 3·3 and 3·4). After off-setting the effect on S_v due to changes in the properties of the organic vehicle during pyrolysis, particle packing in the suspensions investigated is discussed in Section 3.5.

3.3 Thermal expansion

The loss of organic vehicle during pyrolysis causes the linear thermal expansion coefficient (α_L) of samples of test bars to differ from the as-moulded values during cooling and this affects the S_L values calculated. This effect can be corrected for by measuring α_L of core samples of pyrolysed test bars (Table 3) and calculating:

$$(\Delta L)_{exp} = \{(\alpha_L)_{as\text{-}moulded} - (\alpha_L)_{pyrolysed}\}\,\Delta T \quad (2)$$

where $(\Delta L)_{exp}$ is the dimensional change in the test bars due to the change in α_L and ΔT is the difference between the pyrolysis temperature and the room temperature. Since $(\alpha_L)_{as\text{-}moulded} > (\alpha_L)_{pyrolysed}$ at all the temperatures investigated (Table 3), $(\Delta L)_{exp}$ is an expansion. α_L of injection-moulded ceramic bodies shows anisotropy[23] and therefore all measurements were made along the length of the test bars, the direction in which S_L was measured. $(\Delta L)_{exp}$ values were converted to vol.%, $(\Delta V)_{exp}$, using eqn (1) and these results are also presented in Table 3. The maximum error in

Table 3. Coefficient of linear thermal expansion (α_L) of formulations A and B at each pyrolysis temperature and $(\Delta V)_{exp}$ corresponding to the average of the α_L values given

Temperature (°C)	*Formulation A*		*Formulations B*	
	$\alpha_L(MK^{-1})$	$(\Delta V)_{exp}$ *(vol.%)*	$\alpha_L(MK^{-1})$	$(\Delta V)_{exp}$ *(vol.%)*
20 (as moulded)	146, 139, 142	—	134, 147, 152	—
155	133, 110, 120	0·0114	110, 114, 93	0·0156
170	71, 73, 82	0·0303	70, 52, 74	0·0355
195	115, 114, 106	0·0160	95, 105, 107	0·0218
225	59, 51, 60	0·0526	43, 44, 46	0·0614

$(\Delta V)_{exp}$, due to the use of the average α_L values, is 36%. However, these values are of the order 10^{-2} and the actual magnitude of the error involved is extremely small. The error does not change the conclusions of this investigation. In fact, $(\Delta V)_{exp}$ has a negligible effect on particle packing, as described in Section 3.5.

3.4 Crystallinity

DSC results of each sample showed two peaks corresponding to the crystalline melting of microcrystalline wax (MCW) and isotactic polypropylene (IPP). The enthalpies of fusion of 100% crystalline MCW and IPP are 267 J g^{-1} and 165 J g^{-1}, respectively.[24] These values were compared with the measured enthalpies of fusion to calculate the percentage crystallinities of MCW and IPP in each sample (Table 4). These results show that as the test bars were cooled to room temperature, the percentage crystalinity of MCW, in particular, becomes smaller at higher pyrolysis temperatures. The vol.% shrinkage, $(\Delta V)_{crys}$, associated with the crystallinity of MCW and IPP, can be calculated separately using eqn (3):

$$(\Delta V)_{crys} = \text{specific volume change} \times \text{density of MCW (or IPP)} \times \%\ \text{crystallinity} \times \text{vol.\% of MCW (or IPP) in the organic vehicle} \quad (3)$$

The specific volume changes for MCW and IPP are 0·193 $m^3\ Mg^{-1}$ and 0·116 $m^3\ Mg^{-1}$,[24] respectively. The vol.% of MCW and IPP in the organic vehicle was estimated using the relative intensities of the gel permeation chromatograms reported previously[22] and the fact that in the as-moulded state the MCW : IPP weight ratio was 3 : 1 (as mixed proportions). Gel permeation chromatograms also show that in the pyrolysis temperature range investigated the molecular weights of MCW and IPP in the core of the test bars do not change significantly[22] and therefore their as-received densities (given in Section 2.1) were used in calculating the vol.% of the MCW and the IPP in

Table 4. Percentage crystallinity, $(\Delta V)_{crys}$ and $(\Delta V)^*_{crys}$ of formulations A and B at each pyrolysis temperature

Formulation	*Temperature (°C)*	*Percentage crystallinity*		*$(\Delta V)_{crys}$ (vol.%)*			*$(\Delta V)^*_{crys}$ (vol.%)*
		MCW	*IPP*	*MCW*	*IPP*	*Total*	
	20 (as moulded)	33, 40, 37	44, 52, 43	0·76	1·70	2·46	—
	155	31, 36, 30	55, 54, 53	0·50	2·11	2·61	0·15
A	170	23, 30, 24	50, 52, 48	0·41	1·95	2·36	−0·10
	195	22, 24, 25	52, 55, 49	0·39	1·97	2·36	−0·10
	225	13, 20, 21	48, 49, 46	0·26	1·82	2·08	−0·38
B	20 (as moulded)	40, 36, 37	44, 46, 44	0·66	1·42	2·08	—
	155	24, 26, 24	57, 59, 54	0·35	1·86	2·21	0·13
	170	12, 16, 18	48, 50, 53	0·20	1·63	1·83	−0·26
	195	26, 14, 21	50, 50, 50	0·23	1·60	1·83	−0·25
	225	21, 12, 11	43, 36, 41	0·15	1·25	1·40	−0·68

The average percentage crystallinity values were used in the calculations.
A minus sign indicates an expansion.

the organic vehicle and $(\Delta V)_{crys}$ at each pyrolysis temperature.

The organic vehicle also contains approximately 11 wt% of stearic acid which is used as a processing aid.[25] Thermogravimetry of stearic acid shows that at 150°C (approximately the softening point of the formulations) over 50 wt% of the stearic acid is removed. In addition, taking into account processing of the ceramic suspensions in the twin-screw extruder and the injection-moulding machine (Section 2.2), it can be assumed that only a very small amount of stearic acid remains in the formulations at the pyrolysis temperatures investigated and its effect has not been taken into account in the present analysis.

$(\Delta V)_{crys}$ values and the change in $(\Delta V)_{crys}$ at each pyrolysis temperature, compared with the as-moulded samples, $(\Delta V)^*_{crys}$, are also shown in Table 4. The maximum error in $(\Delta V)_{crys}$, due to the use of the average crystallinity values, is 10% and does not change the conclusions of this investigation.

3.5 Particle packing

The measured shrinkage (Table 2) is the sum of the shrinkages caused by particle packing, expansion due to the change in the coefficient of linear thermal expansion coefficient ($(\Delta V)_{exp}$ in Table 3), and the shrinkage (or expansion) due to the change in crystallinity ($(\Delta V)^*_{crys}$ in Table 4). The shrinkage due to particle packing at each pyrolysis temperature calculated on this basis is shown in Fig. 5.

In the as-moulded state of the test bars, all inter-particle space is filled with organic vehicle.[26] Removal of organic vehicle during pyrolysis results in particles moving closer together (particle packing) or the creation of porosity. Previous work[6] has shown that once pyrolysis is complete the vol.% of ceramic in the body could increase only to V^*_{max}, where $V < V^*_{max} < V_{max}$. V is the initial vol.% of ceramic in the suspension and V_{max} is the maximum volume of ceramic that can be incorporated in the suspension and this value is deduced from viscosity data.[27] V^*_{max} is approximately equal to the measured CPVC (critical powder volume concentration) value.[28] Therefore, V^*_{max} represents a situation where the particles move closer to each other and 'lock into position', preventing any further movement.

At 155°C (just above the softening point of the suspensions), when the core of the test bars of both formulations show a 3–4 wt% loss of organic vehicle, calculated particle packing shrinkages are 3·78 vol.% and 2·03 vol.% in formulations A and B, respectively (Fig. 5). However, at 150°C (just below the softening point of the suspensions) when weight loss of organic vehicle is negligible (<1%) the core of the test bars of formulations A and B show measured shrinkages of 2·2 vol.% and 1·6 vol.% respectively (Fig. 4). Relaxation of residual stresses in the test bars caused by injection moulding occurs on heating to the softening point[29] and this can influence the bulk measured shrinkage and particle packing. The more dilute

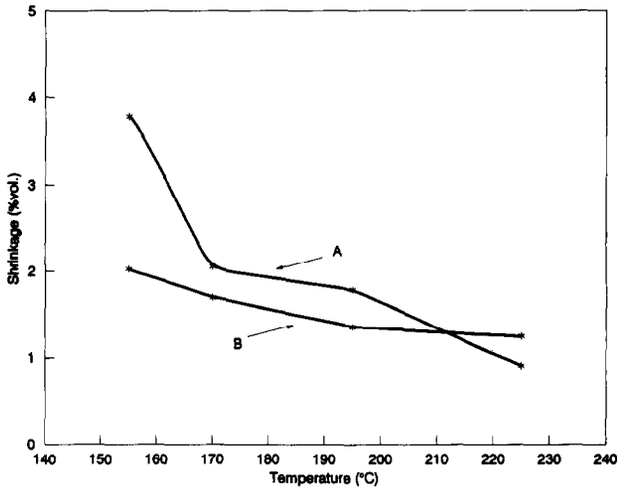

Fig. 5. Variation of shrinkage due to particle packing with pyrolysis temperature in formulations A and B.

formulation A shows a larger initial shrinkage due to particle packing. This is expected as $(V_{max}-V)$ is larger in the case of formulation A. Subsequently, at 170 and 195°C both formulations show a decrease in particle packing in the core of the test bars (Fig. 5). This shows that the volume expansion due to melting of the organic vehicle, which occurs as the temperature exceeds the softening point of the formulations, is not relaxed completely on cooling to room temperature and, in effect, particles are pulled apart. This is despite capillary migration of the MCW from the core of the test bars helping the particles to be drawn towards each other as discussed earlier (see Section 1).

This decrease in particle packing can be explained by considering the interaction between the surface region and the core of each test bar. The surface region loses a larger amount of organic vehicle (Fig. 3) and therefore will experience a greater shrinkage. Previous work[17] has shown that the surface and interconnected porosity remains virtually constant at almost 2–3 vol.% in the temperature range 155–195°C, in both formulations. V^*_{max} of formulations A and B are 51 and 58%, respectively.[6] Taking into account loss of organic vehicle from the surface region (Fig. 3) and neglecting the formation of porosity, the vol.% of ceramic in the surface increases to 54 and 61% (average for the temperature range 155–195°C), in formulations A and B, respectively. Even if the levels of porosity are accounted for completely as surface porosity, the vol.% of ceramic in the surface region is $\simeq V^*_{max}$ of each formulation. Thus, the ceramic particles in the surface region have achieved the maximum packing efficiency and are 'locked together'. This effect makes the surface regions behave like a rigid skin (which appears as a dark degraded region as shown in Fig. 2) and 'holds' the ceramic particles in the core, restraining them from further packing during cooling after being pulled apart due to the volume expansion of the organic vehicle. It can be argued that this type of restraint can lead to cracking. However, cracking was not observed in the present work. The presence of the organic vehicle (>75 wt% remaining in both formulations at 225°C) allows the suspension to behave like a plastic mass, which helps to prevent cracking.

At 225°C, this phenomenon continues to hinder particle packing in formulation A. However, in formulation B, the reduction in particle packing decreases (Fig. 5). This coincides with an increase in the development of porosity in formulation B, as discussed in previous work.[17] Figure 3 shows that in the case of formulation B, compared with formulation A, the rate of weight loss in the core of the test bars is greater and that at 225°C it has lost a higher wt% of the organic vehicle. Therefore, at this temperature, the ceramic particles in formulation B can be expected to pack to a greater extent.

This reduction in particle packing during the early stages of removal of organic vehicle was not observed in previous work.[30,31] In these instances (the same organic vehicle was used), particle packing during interrupted pyrolysis was reported as measured linear shrinkage (uncorrected) and these approached a limiting value at about 190°C. However, a variable rate of heating (much faster than the constant 5°C h^{-1} in the present work) was used to pyrolyse the test bars during the initial stages and a dark skin at the surface of the test bars was not evident. This provides additional evidence for the argument that the extent to which the surface regions form a degraded rigid skin, which seems to be related to the rate of heating during pyrolysis, is an important feature affecting the packing of the ceramic particles during the removal of the organic vehicle. It also indicates that the atmosphere in which pyrolysis takes place will affect shrinkage (and particle packing) in the artefacts. If pyrolysis was carried out in an inert atmosphere such as N_2 where oxidative degradation does not take place, a surface skin which could restrain particle packing in the core of the mouldings would not prevail and larger shrinkages will be observed, as noted by Wright *et al.*[6] Bandyopadhyay & French[8] pyrolysed mouldings in N_2 but their observation of a reduction in shrinkage during the early stages of pyrolysis, as in the present work, was most probably caused by the fact that the mouldings were packed in ceramic powders, which were used as a wicking medium, and this created a restraining effect on the surface.

4 Conclusions

The shrinkage due to the packing of ceramic particles in the core of injection-moulded test bars during the initial stages of pyrolysis in static air has been calculated by correcting measured shrinkage values for changes in the coefficient of thermal expansion and the changes in the crystallinity of the constituents of the organic vehicle. Initially, particle packing increased at a temperature just above the softening point of the formulations but it is likely that the relaxation of residual stresses caused by injection moulding would have influenced shrinkage measurements and affected particle packing. However, subsequent particle packing in the core of the test bars decreased as it was restrained by the rigid surface regions which

form due to oxidative degradation. Comparison of the results of the present work with previous investigations show that the rate of heating and the atmosphere used during pyrolysis also affect particle packing. Although shrinkage due to particle packing in the more concentrated suspension was, as expected, smaller (except at 225°C when there was a steep increase in weight loss compared to the other formulation), there were no major differences in these trends in the two formulations investigated. This indicates that the 7% difference in initial volume fraction of ceramic in the suspensions did not have a significant effect on particle packing during the initial stages of removal of the organic vehicle.

Acknowledgements

The authors wish to thank SERC for financial support given to Ms Shaw during the period 1990–1993. Mr K. K. Dutta is thanked for technical help. The help of Mrs Kathy Goddard in the preparation of this manuscript is gratefully acknowledged.

References

1. Evans, J. R. G., Plastic forming operations for ceramic suspensions. In *New Materials and their Applications*, ed. D. Holland. Institute of Physics, UK 1990, pp. 25–32.
2. Carlsson, R., Shaping of engineering ceramics. *Materials and Design*, **10** (1989) 10–14.
3. Edirisinghe, M. J. & Evans, J. R. G., Review: fabrication of engineering ceramics by injection moulding. II. Techniques. *Int. J. High Technology Ceramics*, **2** (1986) 249–78.
4. Johnson, A., Carlstroem, E., Hermansson, L. & Carlsson, R., Rate controlled thermal extraction of organic binders from injection moulded bodies. *Advances in Ceramics*, **9** (1984) 241–5.
5. Shaw, H. M. & Edirisinghe, M. J., Removal of binder from ceramic bodies fabricated using plastic forming methods. *Bull. Amer. Ceram. Soc.*, **72** (1993) 94–9.
6. Wright, J. K., Edirisinghe, M. J., Zhang, J. G. & Evans, J. R. G., Particle packing in ceramic injection moulding. *J. Am. Ceram. Soc.*, **73** (1990) 2653–8.
7. Kingery, W. D., Densification during sintering in the presence of a liquid phase I. Theory. *J. Appl. Phys.*, **30** (1959) 301–6.
8. Bandyopadhyay, G. & French, K. W., Injection-molded ceramics: Critical aspects of the binder removal process and component fabrication. *J. Eur. Ceram. Soc.*, **11** (1993) 23–34.
9. Barone, M. R. & Ulicny, J. C., Liquid-phase transport during removal of organic binders in injection-moulded ceramics. *J. Amer. Ceram. Soc.*, **73** (1990) 3323–33.
10. Zhang, T., Evans, J. R. G. & Dutta, K. K., Thermal properties of ceramic injection moulding suspensions in the liquid and solid states. *J. Eur. Ceram. Soc.*, **5** (1989) 303–9.
11. German, R. M., *Powder Injection Moulding*. Metal Powder Industries Federation, NJ, USA 1990, p. 301.
12. Shukla, V. N. & Hill, D. C., Binder evolution from powder compacts: thermal profile for injection moulded articles. *J. Amer. Ceram. Soc.*, **72** (1989) 1797–803.
13. Evans, J. R. G. & Edirisinghe, M. J., Interfacial factors affecting the incidence of defects in ceramic mouldings. *J. Mater. Sci.*, **26** (1991) 2081–8.
14. Brydson, J. A., *Plastic Materials*, 5th ed. Butterworth-Heinemann Ltd, London, UK, 1989, pp. 165–7.
15. Wright, D. G. M., Dunk, R., Bouvart, D. & Autran, M., The effect of crystallinity on the properties of injection moulded polypropylene and polyacetal. *Polymer*, **29** (1988) 793–6.
16. Shaw, H. M., Hutton, T. J. & Edirisinghe, M. J., On the formation of porosity during removal of organic vehicle from injection moulded ceramic bodies. *J. Mater. Sci. Lett.*, **11** (1992) 1075–7.
17. Shaw, H. M. & Edirisinghe, M. J., Porosity development during removal of organic vehicle from ceramic injection mouldings. *J. Eur. Ceram. Soc.*, **13** (1994) 135–42.
18. Edirisinghe, M. J. & Evans, J. R. G., Properties of ceramic injection moulding formulations. Part 2. Integrity of mouldings. *J. Mater. Sci.*, **22** (1987) 2267–73.
19. Woodthorpe, J., Edirisinghe, M. J. & Evans, J. R. G., Properties of ceramic injection moulding formulations. III. Polymer removal. *J. Mater. Sci.*, **24** (1989) 1038–48.
20. Wright, J. K., Evans, J. R. G. & Edirisinghe, M. J., Degradation of polyolefin blends used in ceramic injection moulding. *J. Amer. Ceram. Soc.*, **72** (1989) 1822–8.
21. Hansen, R. H., Thermal and oxidative degradation of polyethylene and polypropylene and related olefin polymers. In *Thermal Stability of Polymers*, Vol. 1, ed. R. T. Conley. Marcel Dekker, NY, 1970, pp. 153–87.
22. Shaw, H. M., Edirisinghe, M. J. & Holding, S., Binder degradation and redistribution during pyrolysis of ceramic injection mouldings. *J. Mater. Sci. Lett.*, **12** (1993) 1227–30.
23. Zhang, T. & Evans, J. R. G., Anomalies in the thermal expansion of ceramic injection moulded bodies. *J. Mater. Sci. Lett.*, **9** (1990) 672–4.
24. Wunderlich, B., *Macromolecular Physics*, Vol. 3, *Crystal Melting*, Academic Press Inc. (London) Ltd, 1980, pp. 46–9.
25. Edirisinghe, M. J., The effect of processing additives on the properties of a ceramic–polymer formulation. *Ceramics International*, **17** (1991) 89–96.
26. Wright, J. K. & Evans, J. R. G., Removal of organic vehicle from moulded ceramic bodies by capillary action, *Ceramics International*, **17** (1991) 79–87.
27. Edirisinghe, M. J., Shaw, H. M. & Tomkins, K. L., Flow behaviour of ceramic injection moulding suspensions. *Ceramics International*, **18** (1992) 193–200.
28. Markoff, C. J., Mutsuddy, B. C. & Lennon, J. W., Method of determining critical powder volume concentration in the plastic forming of ceramic mixes. In *Forming of Ceramics*, Vol. 9, ed. J. Mangels & G. L. Messing, American Ceramic Society, OH, USA, 1984, pp. 246–50.
29. Zhang, J. G., Edirisinghe, M. J. & Evans, J. R. G., The use of modulated pressure in ceramic injection moulding. *J. Eur. Ceram. Soc.*, **5** (1989) 63–72.
30. Pinwill, I. E., Edirisinghe, M. J. & Bevis, M. J., Shrinkage during removal of organic vehicle from injection moulded aluminium bodies. *Powder Metallurgy*, **35** (1992) 113–16.
31. Shaw, H. M. & Edirisinghe, M. J., Mobility of powder particles during debinding green ceramic bodies. In *Euro-Ceramics II*, Vol. 1, *Basic Science and Processing of Ceramics*, ed. G. Ziegler & H. Hausner. Deutsche Keramische Gesellschaft e.V., 1991, pp. 423–7.